Proceedings of the 17th World Congress
The International Federation of Automatic Control
Seoul, Korea, July 6-11, 2008

A Novel Clustering Method for Quick Partial Volume Estimation in MR Brain Images

László Szilágyi*,, Sándor M. Szilágyi*,**
Balázs Benyó, Zoltán Benyó****

** Faculty of Technical and Human Sciences, Sapientia – Hungarian Science University of Târgu-Mureş, Romania (Tel: +40-747-352560; e-mail: {lalo,szs}@ sapientia.ro).*
*** Department of Control Engineering and Information Technology, Budapest University of Technology and Economics, Budapest, Hungary (e-mail: benyo@mit.bme.hu, benyo@iit.bme.hu)*

Abstract: Automated brain MR image segmentation is a challenging pattern recognition problem that received significant attention lately. The most popular solutions involve fuzzy c-means (FCM) or similar clustering mechanisms. Several improvements have been made to the standard FCM algorithm, in order to reduce its sensitivity to Gaussian, impulse, and intensity non-uniformity noises. This paper presents a modified FCM-based method that targets accurate and fast segmentation in case of mixed noises. The proposed method extracts a scalar feature value from the neighbourhood of each pixel, using a context dependent filtering technique that deals with both spatial and grey level distances. These features are clustered afterwards by the histogram-based approach of the enhanced FCM algorithm. Results were evaluated based on synthetic phantoms and real MR images. Test experiments revealed that the proposed method provides better results compared to other reported FCM-based techniques. The time complexity of the proposed method is situated well below the traditional FCM algorithm. The achieved segmentation and the obtained fuzzy membership values represent excellent support for deformable contour model based cortical surface reconstruction methods.

1. INTRODUCTION

The segmentation of an image represents the separation of its pixels into non-overlapping, consistent regions, which appear to be homogeneous with respect to some criteria concerning grey level intensity and/or texture.

The fuzzy c-means (FCM) algorithm is one of the most widely used method for data clustering, and probably also for brain image segmentation (Bezdek and Pal, 1991). However, in this latter case, standard FCM is not efficient by itself, as it fails to deal with that significant property of images, that neighbour pixels are strongly correlated. Ignoring this specificity leads to strong noise sensitivity and several other imaging artefacts.

Recently, several solutions were given to improve the performance of segmentation. Most of them involve using local spatial information: the own grey level of a pixel is not the only information that contributes to its assignment to the chosen cluster. Its neighbours also have their influence while getting a label. Pham and Prince (1999) modified the FCM objective function by including a spatial penalty, enabling the iterative algorithm to estimate spatially smooth membership functions. Ahmed *et al.* (2002) introduced a neighbourhood averaging additive term into the objective function of FCM, calling the algorithm bias corrected FCM (BCFCM). This approach has its own merits in bias field estimation, but it gives the algorithm a serious computational load by computing the neighbourhood term in every iteration step. Moreover, the zero gradient condition at the estimation of the bias term produces a significant amount of misclassifications (Siyal and Yu, 2005). Chuang *et al.* (2006) proposed averaging the fuzzy membership function values over a predefined neighbourhood and reassigning them according to a trade-off between the original and averaged membership values. This approach can produce accurate clustering if the trade-off is well adjusted empirically, but it is enormously time consuming.

Aiming at reducing the execution time, Szilágyi *et al.* (2003), and Chen and Zhang (2004) proposed to evaluate the neighbourhoods of each pixel as a pre-filtering step, and perform FCM afterwards. The averaging and median filters, followed by FCM clustering, are referred to as FCM_S1 and FCM_S2, respectively (Chen and Zhang, 2004). Once having the neighbours evaluated, and thus having extracted a scalar feature value for each pixel, FCM can be performed on the basis of the grey level histogram, clustering the grey levels instead of the pixels, causing a significant reduction of the computational load, as the number of grey levels is generally smaller by orders of magnitude (Szilágyi *et al.*, 2003). This latter quick approach, combined with an averaging pre-filter, is referred to as enhanced FCM (EnFCM). All BCFCM, FCM S1, and EnFCM suffer from the presence of a parameter denoted by, which controls the strength of the averaging effect, balances between the original and averaged image, and whose ideal value unfortunately can be found only experimentally. Another disadvantage emerges from the fact, that averaging and median filters, besides eliminating salt-and-pepper and Gaussian noises, also blur relevant edges. Due to these shortcomings, Cai *et al.* (2007) introduced a new local similarity measure, combining spatial and grey level distances, and applied it as an alternative pre-filtering to EnFCM, calling this approach fast generalized FCM (FGFCM). This approach is able to extract local information causing less blur than the averaging or median filters, but failed to eliminate the experimentally adjusted parameter, denoted here by λ_g, which controls the effect of grey level differences.

In this paper we propose a novel method for MR brain image segmentation that simultaneously targets high accuracy in image segmentation, low noise sensitivity, and high processing speed. The remainder of the paper is organized as follows. Section 2 gives a detailed presentation of background works, including standard and spatially constrained FCM. Section 3 deals with the proposed context sensitive filtering and segmentation method. Some considerations regarding partial volume artefacts also exhibited here. The performance evaluation via experimental comparison is presented in Section 4, while Section 5 gives conclusions and several topics for future works.

2. BACKGROUND

The fuzzy c-means algorithm has successful applications in a wide variety of clustering problems. The traditional FCM partitions a set of object data into a number of c clusters based on the minimization of a quadratic objective function. When applied to segment grey level images, FCM clusters the scalar intensity level of all pixels $(x_k, k=1...n)$. The objective function to be minimized is:

$$J_{FCM} = \sum_{i=1}^{c}\sum_{k=1}^{n} u_{ik}^{m}(x_k - v_i)^2, \quad (1)$$

where $m>1$ is the fuzzyfication parameter, v_i represents the prototype value of cluster i, $u_{ik} \in [0,1]$ is the fuzzy membership function showing the degree to which pixel k belongs to cluster i. According to the definition of fuzzy sets, for any pixel k, we have $\sum_{i=1}^{c} u_{ik} = 1$. The minimization of the objective function is reached by alternately applying the optimization of J_{FCM} over $\{u_{ik}\}$ with v_i fixed, $i=1...c$, and the optimization of J_{FCM} over $\{v_i\}$ with u_{ik} fixed, $i=1...c$, $k=1...n$ (Hathaway *et al.*, 2000). During each cycle, the optimal values are computed from the zero gradient conditions, and obtained as follows:

$$u_{ik}^{*} = \frac{(x_k - v_i)^{-2/(m-1)}}{\sum_{j=1}^{c}(x_k - v_j)^{-2/(m-1)}} \quad \forall i=1...c, \forall k=1...n, \quad (2)$$

$$v_i^{*} = \frac{\sum_{k=1}^{n} u_{ik}^{m} x_k}{\sum_{k=1}^{n} u_{ik}^{m}} \quad \forall i=1...c. \quad (3)$$

FCM has invaluable merits in making optimal clusters, but in image processing it has severe deficiencies, such as failing to take into consideration the position of pixels, which is also relevant information in image segmentation. This drawback led to introduction of spatial constraints into fuzzy clustering.

Ahmed *et al.* (2002) proposed a modification to the objective function of FCM, in order to allow the labelling of a pixel to be influenced by its immediate neighbours. This neighbouring effect acts like a regularizer that biases the solution to a piecewise homogeneous labelling. The objective function of BCFCM is:

$$J_{BCFCM} = \sum_{i=1}^{c}\sum_{k=1}^{n}\left[u_{ik}^{m}(x_k - v_i)^2 + \frac{\alpha}{n_k}\sum_{r \in N_k} u_{ik}^{m}(x_r - v_i)^2\right], \quad (4)$$

where x_r represents the grey level of pixels situated in the neighbourhood N_k of pixel k, and n_k is the cardinality of N_k. The parameter α controls the intensity of the neighbouring effect, and unfortunately its optimal value can be found only experimentally. Having the neighbourhood averaging terms computed in every computation cycle, this iterative algorithm performs extremely slowly.

Chen and Zhang (2004) reduced the time complexity of BCFCM, by previously computing the neighbouring averaging term or replacing it by a median filtered term, calling these algorithms FCM_S1 and FCM_S2, respectively. These algorithms outperformed BCFCM, at least from the point of view of time complexity.

Szilágyi *et al.* (2003) proposed a regrouping of the processing steps of BCFCM. In their approach, an averaging filter is applied first, similarly to the neighbouring effect of Ahmed *et al.* (2002):

$$\xi_k = \frac{1}{1+\alpha}\left(x_k + \frac{\alpha}{n_k}\sum_{r \in N_k} x_r\right), \quad (5)$$

followed by an accelerated version of FCM clustering. The acceleration is based on the idea, that the number of grey levels is generally much smaller than the number of pixels. In this order, the histogram of the filtered image is computed, and not the pixels, but the grey levels are clustered (Szilágyi *et al.*, 2003), by minimizing the following objective function:

$$J_{EnFCM} = \sum_{i=1}^{c}\sum_{l=1}^{q} h_l u_{il}^{m}(l - v_i)^2, \quad (6)$$

where h_l denotes the number of pixels with grey level equalling l, and q is the number of grey levels. The optimization formulas in this case will be:

$$u_{il}^{*} = \frac{(l - v_i)^{-2/(m-1)}}{\sum_{j=1}^{c}(l - v_j)^{-2/(m-1)}} \quad \forall i=1...c, \forall l=1...q, \quad (7)$$

$$v_i^{*} = \frac{\sum_{k=1}^{n} h_l u_{il}^{m} l}{\sum_{k=1}^{n} h_l u_{il}^{m}} \quad \forall i=1...c. \quad (8)$$

EnFCM drastically reduces the computation complexity of BCFCM and its relatives (Szilágyi *et al.*, 2003; Cai *et al.*, 2007). If the averaging pre-filter is replaced by a median filter, the segmentation accuracy also improves significantly (Szilágyi, 2006; Cai *et al.*, 2007).

Based on the disadvantages of the aforementioned methods, but inspired of their merits, Cai *et al.* (2007) introduced a local (spatial and grey) similarity measure that they used to compute weighting coefficients for an averaging pre-filter. The filtered image is then subject to EnFCM-like histogram-based fast clustering. The similarity between pixels k and r is given by the following formula:

$$S_{kr} = \begin{cases} s_{kr}^{(s)} \cdot s_{kr}^{(g)} & r \in N_k, r \neq k \\ 0 & r = k \end{cases}, \tag{9}$$

where $s_{kr}^{(s)}$ and $s_{kr}^{(g)}$ are the spatial and grey level components, respectively. The spatial term $s_{kr}^{(s)}$ is defined as the L_∞-norm of the distance between pixels k and r. The grey level term is computed as

$$s_{kr}^{(g)} = \exp\left[-(x_k - x_r)^2 / (\lambda_g \sigma_k^2)\right], \tag{10}$$

where σ_k^2 denotes the average quadratic grey level distance between pixel k and its neighbours. Segmentation results are reported to be more accurate than in any previously presented case (Cai *et al.*, 2007).

3. METHODS

Probably the most relevant problem of all techniques presented above, BCFCM, EnFCM, FCM_S1, and FGFCM, is the fact that they depend on at least one parameter, whose value has to be adjusted experimentally.

The zero value in the second row of Eq. (9) implies that in FGFCM, the filtered grey level of any pixel is computed as a weighted average of its neighbour pixel intensities. Having renounced to the original intensity of the current pixel, even if it is a reliable, noise-free value, unavoidably produces some extra blur into the filtered image. Accurate segmentation requires this kind of effects to be minimized (Pham, 2003).

3.1 Context Dependent Filtering

In this paper we propose a set of modifications to EnFCM/FGFCM, in order to improve the accuracy of segmentation, without renouncing to the speed of histogram-based clustering. In other words, we need to define a complex filter that can extract relevant feature information from the image while applied as a pre-filtering step, so that the filtered image can be clustered fast afterwards based on its histogram. The proposed method consists of the following steps:

A. As we are looking for the filtered value of pixel k, we need to define a small square or diamond-shape neighbourhood N_k around it. Square windows of size 3×3 and 5×5 were used throughout this study, but other window sizes and shapes are also possible.

B. We search for the minimum, maximum, and median grey value within the neighbourhood N_k, and we denote them by $\min_k$, $\max_k$ and med_k, respectively.

C. We replace the grey level of the maximum and minimum valued pixel with the median value (if there are more than one maxima or minima, replace them all), unless they are situated in the middle pixel k. In this latter case, pixel k remains unchanged, just labelled as unreliable value.

D. Compute the average quadratic grey level difference of the pixels within the neighbourhood N_k, using the formula

$$\sigma_k = \sqrt{\frac{\sum_{r \in N_k - \{k\}} (x_r - x_k)^2}{n_k - 1}}. \tag{11}$$

E. The filter coefficients will be defined as:

$$C_{kr} = \begin{cases} c_{kr}^{(s)} \cdot c_{kr}^{(g)} & r \in N_k - \{k\} \\ 1 & r = k, x_k \notin \{\max_k, \min_k\} \\ 0 & r = k, x_k \in \{\max_k, \min_k\} \end{cases}. \tag{12}$$

The central pixel k will have coefficient 0 if its value was found unreliable, otherwise it has unitary coefficient. All other neighbour pixels will have coefficients $C_{kr} \in [0,1]$, depending on their space distance and grey level difference from the central pixel. In case of both terms, higher distance values will push the coefficients towards 0.

F. The spatial component $c_{kr}^{(s)}$ is a negative exponential of the Euclidean distance between the two pixels k and r: $c_{kr}^{(s)} = \exp(-L_2(k,r))$. The grey level term is defined as follows:

$$c_{kr}^{(g)} = \begin{cases} \frac{1}{2}\left[1 + \cos\left(\pi \frac{x_r - x_k}{4\sigma_k}\right)\right] & |x_r - x_k| \leq 4\sigma_k \\ 0 & |x_r - x_k| > 4\sigma_k \end{cases}. \tag{13}$$

The above function has a bell-like shape within the interval $[-4\sigma_k, 4\sigma_k]$, and is constant zero outside the interval.

G. The extracted feature value for pixel k, representing its filtered intensity value, is obtained as a weighted average of its neighbours:

$$\xi_k = \frac{\sum_{r \in N_k} C_{kr} x_r}{\sum_{r \in N_k} C_{kr}} \tag{14}$$

The algorithm can be summarized as follows:

1. Pre-filtering step: for each pixel k of the input image, compute the filtered grey level value ξ_k, using (11), (12), (13), and (14).

2. Compute the histogram of the pre-filtered image, obtain the values h_l, $l = 1...q$.

3. Initialize v_i with valid grey level values, differing from each other, $i = 1...c$.

4. Compute new u_{il} fuzzy membership values, using (7).

5. Compute new v_i prototype cluster values, using (8).

6. If there is relevant change in the v_i values, go back to step 4. This is tested by comparing any norm of the difference between the new and the old vector $\mathbf{v}$ with a preset small constant ε.

The algorithm converges quickly, however, the number of necessary iterations depends on ε and on the initial cluster prototype values.

3.2 Partial Volume Estimation

Whatever resolution an MR scanner may have, the scanned images will contain such pixels where more than one tissue classes are present. This phenomenon is referred to as partial volume effect (PVE). Although it is not granted, it is reasonable to assume that within a given pixel, PVE only occurs over two classes (Pham and Prince, 1998). Pixels involved in PVE are generally modelled using the mixel model (Ruan *et al.*, 2000), which states that the grey level intensity of pixel k is given by:

$$x_k = \alpha_k v_\mu + (1-\alpha_k) v_\nu + \eta_k \, , \qquad (15)$$

where η_k represents the noise of pixel k that will be ignored after context dependent filtering, while v_μ and v_ν are the centroids of the two involved classes, assuming $v_\mu \le x_k \le v_\nu$.

Fuzzy membership values given by FCM-based clustering techniques are reported to give a good estimate of the partial volumes (Zhang *et al.*, 2001). Let us inspect now on theoretical basis, under what circumstances will the fuzzy memberships satisfy (15). In this order, we would like to have

$$\frac{u_{\mu k}}{u_{\nu k}} = \frac{\alpha_k}{1-\alpha_k} \, . \qquad (16)$$

By combining (2) and (15), we obtain

$$\frac{u_{\mu k}}{u_{\nu k}} = \left(\frac{x_k - v_\mu}{v_\nu - x_k} \right)^{\frac{-2}{m-1}} = \left(\frac{(1-\alpha_k)(v_\nu + v_\mu)}{\alpha_k (v_\nu + v_\mu)} \right)^{\frac{-2}{m-1}} = \left(\frac{\alpha_k}{1-\alpha_k} \right)^{\frac{2}{m-1}} \qquad (17)$$

which equals the desired value shown in (16) if and only if $m = 3$.

Consequently, if FCM is required to give estimation of partial volume ratios, the usage of fuzzification exponent $m = 3$ is recommendable.

4. RESULTS AND DISCUSSION

In this section we test and compare the accuracy of four algorithms: BCFCM, EnFCM, FGFCM, and the proposed method, on several synthetic and real images. All the following experiments used 3×3 or 5×5 window size for all kinds of filtering.

The proposed filtering technique uses a convolution mask, whose coefficients are context dependent and thus computed for the neighbourhood of each pixel. Fig. 1 presents the obtained coefficients for two particular cases. Fig. 1(a) shows the case, when the central pixel is not significantly noisy, but some pixels in the neighbourhood might be noisy or might belong to a different cluster. Under such circumstances, the three pixels on the left side having distant grey level compared to the value of the central pixel, receive small weights and this way they hardly contribute to the filtered value. Fig. 1(b) presents the case of an isolated noisy pixel situated in the middle of a relatively homogeneous window. Even though all computed coefficients are low, the noise is eliminated, leading to a convenient filtered value 76. The arrow-indicated migration of weights from the local maximum and minimum towards the median valued pixel, caused by step C of the filtering method, is relevant in the second case and useful in the first.

107 0.2577	40 0.0000	46 0.5128
113 0.3073	43 1.0000	47 1.9418
116 0.0000	41 0.7161	49 0.5107

(a)

67 0.0000	72 0.0668	76 0.0645
73 0.0723	169 0.0000	85 0.1523
75 0.0601	70 0.0564	74 0.1118

(b)

Fig. 1. Filter mask coefficients in case of a reliable pixel intensity value (a), and a noisy one (b). The upper number in each cell represents the intensity value, while the lower number shows the obtained weight. The arrows indicate that the coefficients of extreme intensities are contributed to the median valued pixel.

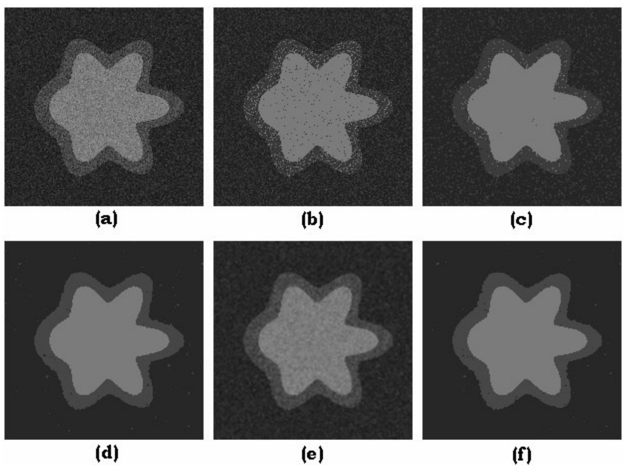

Fig. 2. Segmentation results on phantom images: (a) original, (b) segmented with traditional FCM, (c) segmented using BCFCM, (d) segmented using FGFCM, (e) filtered using the proposed pre-filtering, (f) result of the proposed segmentation.

Fig. 3 shows the evolution of misclassifications obtained using three of the presented methods, while segmenting the phantom shown in Fig. 2(a), corrupted by an increasing amount of mixed noise (Gaussian noise, salt-and-pepper impulse noise, and mixtures of these). Moreover, not only an extra amount of noise is added to the image step by step, but also the original cluster centroids (the base intensities of the clusters) are moved closer and closer to each other. This complex effect is obtained using a variably weighted sum of three different noisy versions of the same image (all available at Internet Brain Segmentation Repository (Worth, 2000)). Fig. 3 reveals that the proposed filter performs best at removing all these kinds of noises. Consequently, the proposed method is suitable for segmenting images corrupted with unknown noises, and in all cases it performs at least as well as his ancestors.

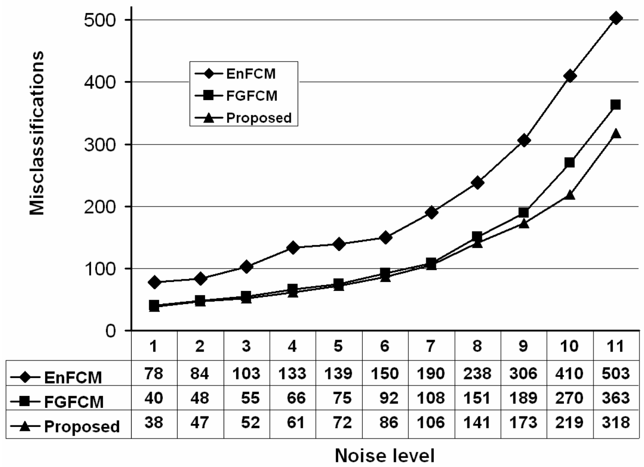

Fig. 3. A comparison of the numbers of misclassifications at rising noise level (from left to right).

Table 1. Misclassification rates in case of real brain MR image segmentation

Noise	EnFCM	FGFCM	Proposed
Original	0.767%	0.685%	0.685%
Gaussian 4%	1.324%	1.131%	1.080%
Gaussian 12%	4.701%	2.983%	2.654%
Impulse 3%	1.383%	0.864%	0.823%
Impulse 5%	1.916%	1.227%	0.942%
Impulse 10%	3.782%	1.268%	1.002%
Gaussian 4% + Impulse 5%	2.560%	1.480%	1.374%
Gaussian 12% + Impulse 5%	6.650%	4.219%	4.150%

We applied the presented filtering and segmentation techniques to several T1-weighted real MR images. A detailed view, containing numerous segmentations, is presented in Fig. 4. The original slice (a) is taken from IBSR. We produced several noisy versions of this slice, by artificially adding salt-and-pepper impulse noise and/or Gaussian noise, at different intensities. Some of these noisy versions are visible in Fig. 4 (d), (g), (j), (m). The filtered versions of the five above mentioned slices are presented in the middle column of Fig. 4. The segmentation results are shown in Fig. 4 (c), (f), (i), (l), (o), accordingly. From the segmented images we can conclude, that the proposed filtering technique is efficient enough to make proper segmentation of any likely-to-be-real MRI images in clinical practice, at least from the point of view of Gaussian and impulse noises.

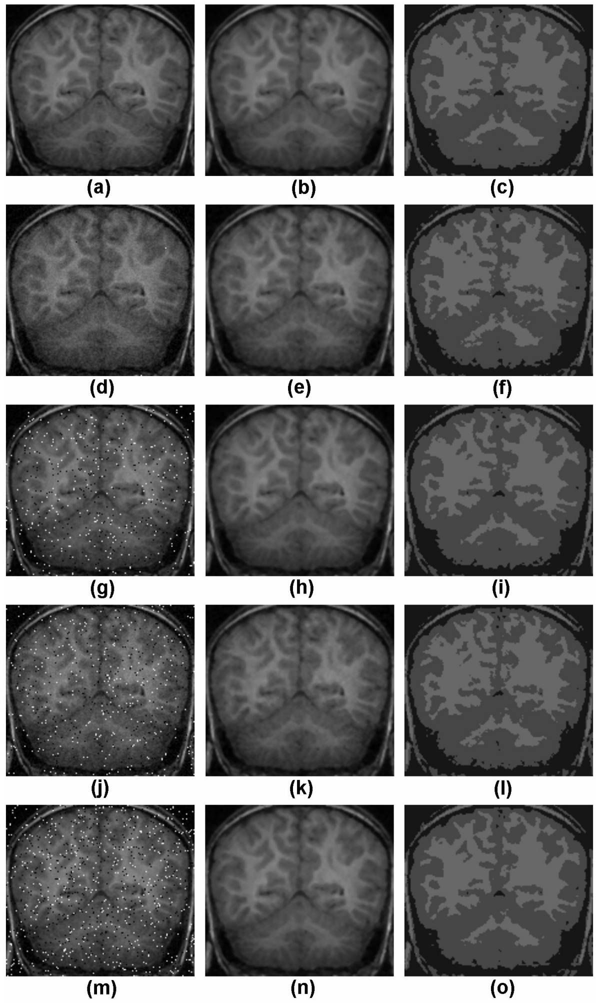

Fig. 4. Filtering and segmentation results on real T1-weighted MR brain images, corrupted with different kinds and levels of artificial noise. Each row contains an original or noise-corrupted brain slice on the left side, the filtered version (using the proposed method) in the middle, and the segmented version on the right side. Row (a)-(c) comes from record number 1320_2_43 of IBSR, row (d)-(f) is corrupted with 10% Gaussian noise, while rows (g)-(i), (j)-(l), and (m)-(o) contain mixed noise of 3% impulse + 5% Gaussian, 3% impulse + 10% Gaussian, and 5% impulse + 5% Gaussian, respectively.

Table 1 takes into account the behaviour of three mentioned segmentation techniques, in case of different noise types and intensities, computed by averaging the misclassifications on 12 different T1-weighted real MR brain slices. The proposed algorithm has lowest misclassification rates in most of the cases.

Fig. 5 presents one slice of real, T2-weighted MR brain image, and its segmentation using the proposed method. Visual inspection shows, that our segmentation results are very close to the IBSR expert's manual inspection.

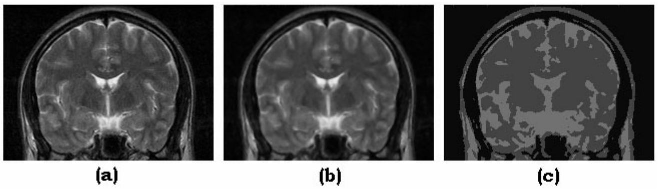

Fig. 5. Segmentation results on real T2-weighted MR images: (a) original, (b) filtered using the proposed method, (c) result of the proposed segmentation.

The efficiency of the algorithm against the clock is mainly assured by the histogram-based execution of the fuzzy c-means clustering. As the number of grey intensities of an MRI image is well under the number of voxels present in a single slice or a stack of parallel slices ($q \ll n$), the time complexity of the segmentation is reduced from $O(cnz)$ to $O(cqz)$, where z represents the number of executed cycles. Taking the computation of the histogram and the proposed pre-filtering into account, even though the proposed filter is obviously 7–8 times slower than a fixed low-pass averaging or a simple 3×3 median filter, we still have a 10–20 times speed-up compared to the execution of the standard FCM algorithm.

We applied the proposed segmentation method to several complete head MR scans in IBSR. The dimensions of the image stacks were 256×256×64 voxels. The average total processing time for one stack was around 10 seconds on a 2.4 GHz Pentium 4.

5. CONCLUSIONS

We have developed a modified FCM algorithm for automatic segmentation of MR brain images. The algorithm was presented as a combination of a context dependent pre-filtering technique and an accelerated FCM clustering performed over the histogram of the filtered image. The pre-filter uses both spatial and grey level criteria, in order to efficiently eliminate Gaussian and impulse noises without significantly blurring the real edges.

Several test series were carried out using synthetic brain phantoms and real MR images. These investigations revealed, that our proposed technique accurately segments the different tissue classes under serious noise contamination.

We compared our results with other recently reported methods. Test results revealed that our approach outperformed these methods in many aspects, especially in the accuracy of segmentation and processing time.

Further works target more precise treatment of partial volume artefacts, removal of intensity non-uniformity noises, and adaptive determination of the optimal number of clusters.

REFERENCES

Ahmed, M.N., S.M. Yamany, N. Mohamed and A.A. Farag (2002). A Modified Fuzzy C-Means Algorithm for Bias Field Estimation and Segmentation of MRI Data. *IEEE Trans. Med. Imag.,* **21**, 193-199.

Bezdek, J.C. and S.K. Pal (1991). *Fuzzy Models for Pattern recognition*. IEEE Press, Piscataway, NJ.

Cai, W., S. Chen, and D.Q. Zhang (2007). Fast and robust fuzzy c-means algorithms incorporating local information for image segmentation. *Patt. Recogn.,* **40**, 825–838.

Chen, S., and D.Q. Zhang (2004). Robust image segmentation using FCM with spatial constraints based on new kernel-induced distance measure. *IEEE Trans. Syst. Man Cybern. Part B.,* **34**, 1907–1916.

Chuang, K.S., H.L. Tzeng, S. Chen, J. Wu, and T.J. Chen (2006). Fuzzy c-means clustering with spatial information for image segmentation. *Comp. Med. Imag. Graph.,* **30**, 9–15.

Hathaway, R.J., J.C. Bezdek, and Y. Hu (2000). Generalized fuzzy c-means clustering strategies using L_p norm distances. *IEEE Trans. Fuzzy. Syst.,* **8**, 576–582.

Pham, D.L., and J.L. Prince (1998). Partial volume estimation and the fuzzy c-means algorithm. *Proc. Int. Conf. Imag. Proc.,* 819-822.

Pham, D.L., and J.L. Prince (1999). Adaptive fuzzy segmentation of magnetic resonance images. *IEEE Trans. Med. Imag.,* **18**, 737-752.

Pham, D.L. (2003). Unsupervised tissue classification in medical images using edge-adaptive clustering. *Proc. Ann. Int. Conf. IEEE EMBS,* **25,** 634–637.

Ruan, S., C. Yaggi, J.H. Xue, M.J. Fadili, and D. Bloyet (2000). Brain tissue classification of magnetic resonance images using partial volume modeling. *IEEE Trans. Med. Imag.,* **19**, 1179-1187.

Siyal, M.Y. and L. Yu (2005). An Intelligent Modified Fuzzy C-Means Based Algorithm for Bias Field Estimation and Segmentation of Brain MRI. *Patt. Recogn. Lett.,* **26,** 2052–2062.

Szilágyi, L., Z. Benyó, S. M. Szilágyi, and H. S. Adam (2003). MR brain image segmentation using an enhanced fuzzy c-means algorithm. *Proc. Ann. Int. Conf. IEEE EMBS,* **25,** 724–726.

Szilágyi, L. (2006). Medical Image Processing Methods for the Development of a Virtual Endoscope. *Periodica Polytechnica Ser. El. Eng.,* **50,** 69-78.

Worth, A (2000) Internet Brain Segmentation Repository. http://www.cma.mgh.harvard.edu/ibsr.

Zhang, Y., M. Brady, and S. Smith (2001). Segmentation of brain MR images through a hidden Markov random field model and the expectation-maximization algorithm. *IEEE Trans. Med. Imag.,* **20,** 45–57.